ACS Photonics

Article

pubs.acs.org/journal/apchd5

Hot Electron Photoemission from Plasmonic Nanostructures: The Role of Surface Photoemission and Transition Absorption

Viktoriia E. Babicheva,*[,†,‡] Sergei V. Zhukovsky,[†,§] Renat Sh. Ikhsanov,[∥] Igor E. Protsenko,[⊥,#] Igor V. Smetanin,[⊥] and Alexander Uskov*[,†,⊥,#]

[†]ITMO University, Kronverkskiy 49, 197101, St. Petersburg, Russia

[‡]Center for Nano-Optics, Georgia State University, P.O. Box 3965, Atlanta, Georgia 30302, United States

[§]DTU Fotonik, Technical University of Denmark, Oersteds Plads 343, 2800, Kgs. Lyngby, Denmark

[∥]Research Institute of Scientific Instruments, State Nuclear Energy Corporation "Rosatom", Moscow, Russia

[⊥]P. N. Lebedev Physical Institute, Leninskiy Prospect 53, 119991, Moscow, Russia

[#]Advanced Energy Technologies Ltd, Skolkovo, Novaya Ulica 100, 143025, Moscow Region, Russia

ABSTRACT: We study mechanisms of photoemission of hot electrons from plasmonic nanoparticles. We analyze the contribution of "transition absorption", i.e., loss of energy of electrons passing through the boundary between different materials, to the surface mechanism of photoemission. We calculate photoemission rate and transition absorption for nanoparticles surrounded by various media with a broad range of permittivities and show that photoemission rate and transition absorption follow the same dependence on the permittivity. Thus, we conclude that transition absorption is responsible for the enhancement of photoemission in the surface scenario. We calculate the ratio of photoemission cross-section for a gold nanosphere embedded in different materials such as silicon, zinc oxide, and titanium dioxide. For the calculations, we include both surface and bulk mechanisms of photoemission, using quantum calculations for the former one and a three-step phenomenological approach for the latter one. By comparison of both mechanisms, we show that the role of surface mechanism in the total photoemission cannot be neglected, as it dominates in the near-infrared wavelength range. We also show that in order to increase the photoemission rate, one benefits from placing nanoparticles in materials with lower permittivity. Finally, we apply our results to the case of nanowires partially embedded in a semiconductor substrate, which is a practically relevant design for narrow-band photodetection. Summarizing these results, we show that the reported narrow-band photoemission increase can at least partially be attributed to the surface mechanism.

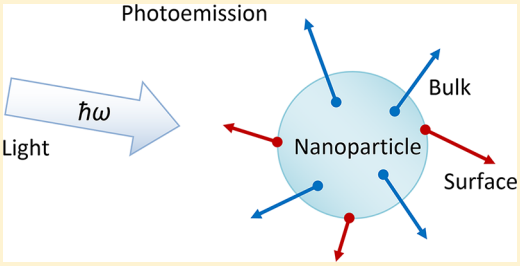

KEYWORDS: *hot electron photoemission, plasmonic nanostructures, surface photoelectric effect, volume photoelectric effect, transition absorption*

Utilizing plasmonic nanoparticles, or more generally, plasmonic nanoantennas, can increase the efficiency of light−matter interaction, as they allow high field localization and enhancement. In particular, plasmonic nanoparticles and nanowires can cause intensive generation of hot photoelectrons (Figure 1a) and consequently be utilized for more efficient conversion of solar energy in photovoltaic devices,[1−6] as well as in photodetectors[7−12] and photocatalysis.[13−17]

It has long been known that, in general, the rate of any photoemission process strongly depends on the photon energy (i.e., spectral region), particle shape, and materials involved. Dating back to 1931, two underlying physical mechanisms of photoemission were defined:[18] (A) A *bulk* or *volume* mechanism occurs when an electron absorbs a photon inside the metal (three-body collision is required, so phonons or impurities are involved). To describe a bulk mechanism,[19] one can usually apply a three-step phenomenological model: (i) an electron absorbs photon energy and becomes "hot"; (ii) it moves to the boundary (most likely losing energy in the process); and (iii) if its energy is sufficient, the electron is emitted outside through the boundary. For the case of a nanoparticle with the Schottky barrier at the boundary, the diagram of such a photoemission process is shown in Figure 1b. Each of the steps (i)−(iii) can be considered independently, so the transition probability is simply a product of the probabilities for the three steps. In the bulk mechanism, the photoemission rate is proportional to the local light absorption rate in the bulk metal. (B) A *surface* mechanism occurs when an electron absorbs a photon at the collision with the metal surface (which plays the role of the third body) and is then emitted from the metal if the electron acquires enough energy (Figure 1c). The concept of surface mechanism was proposed back in 1931,[18] and further theory was developed in a full quantum approach.[20−24] In the surface mechanism, the rate of photo-

Received: February 11, 2015
Published: July 10, 2015

DOI: 10.1021/acsphotonics.5b00059
ACS Photonics 2015, 2, 1039−1048

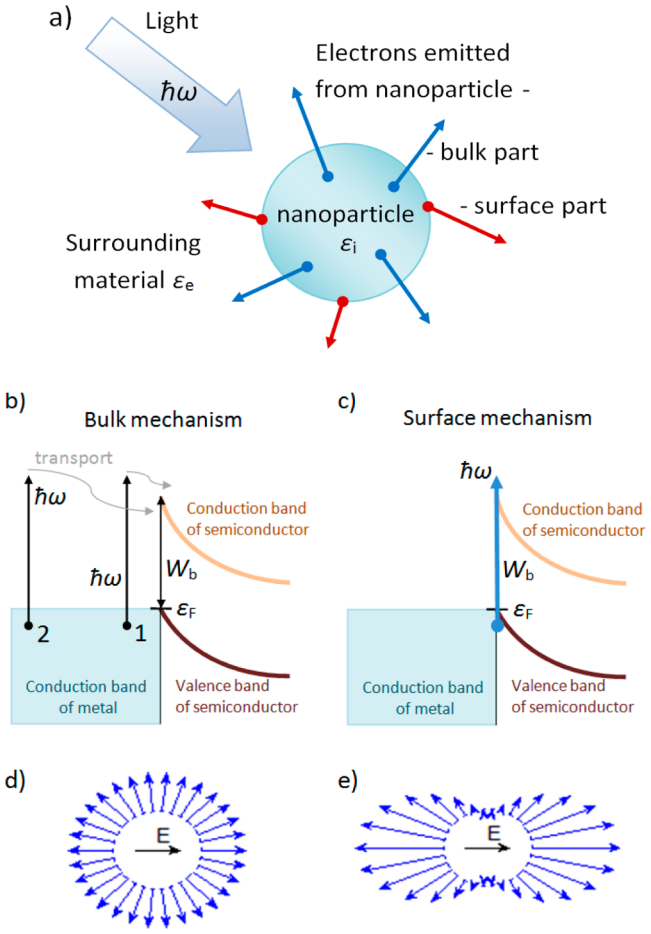

Figure 1. (a) Schematic view of a metal nanoparticle and photoemission of hot electrons under light illumination. Two mechanisms of photoemission of hot electrons are considered. (b) Bulk photoemission: electron 1 receives energy $\hbar\omega > W_b$, moves to the Schottky barrier, and overcomes it, leaving the metal; electron 2 does not have enough energy when it reaches the barrier, so it remains in the metal. (c) Surface photoemission: an electron collides with the Schottky barrier, absorbs the photon $\hbar\omega > W_b$, and leaves the metal. W_b is the work function for the metal/semiconductor interface; ε_F is the Fermi level. Bulk and surface mechanisms of photoemission possess different angular distributions: (d) It is uniform for the bulk mechanism, but (e) highly directional for the surface one (small-particle and quasistatic approximation are assumed).

emission from the metal is proportional to the square of the electromagnetic field component normal to the metal surface.

The interest in this topic was rekindled when it was realized that hot electrons can be excited by strong local fields appearing at the resonant excitation of surface plasmon polaritons (referred to as simply *plasmons* for short) in metal nanoparticles.[25−29] During this decade, an extensive experimental study of photoemission from such "plasmonic" nanoparticles was carried out. For example, the successful experimental demonstration of enhanced photoemission in plasmonic nanoparticle arrays was recently performed with the focus on Schottky barrier detectors.[9]

It should be noted that in a plasmonic resonance involving a nanoparticle both the electric field absorbed inside the particle and the outside electric field near the nanoparticle surface, contributing to the bulk and surface mechanisms, respectively, are enhanced simultaneously. Consequently, the experimentally measured photoemission increase follows the increase in the extinction cross-section of the particle related to both mechanisms. For this reason, most of the recent works on plasmonic photoemission do not specify which mechanism is mostly responsible for the photoemission. It often happens that both mechanisms give comparable contributions to the photoemission. For example, by experimental comparison of the bulk and the surface photoemission mechanisms, it was shown that about 35% of the yield under surface plasmon excitation on 20 nm thick aluminum film could be accounted for by the bulk mechanism.[25]

However, even though both mechanisms benefit from the field enhancement caused by the plasmonic resonance excitation, it is important to be able to account for each of them correctly in order to find optimal conditions for both.

Furthermore, being able to discriminate between the two mechanisms becomes important when finer properties of photoemission need to be studied. For example, there is a substantial difference in the directionality diagram of the emitted electrons. In the simplest case of a spherical nanoparticle, the hot electron motion in the bulk mechanism is completely isotropic, at least in the approximation employed in refs 30 and 31. Consequently, hot electrons are emitted from the particle in all directions (Figure 1d). In contrast, in the surface mechanism the photoemission rate is proportional to the square of the component of the electric field normal to the boundary,[21] so the emission is much higher in the direction of the electric field polarization (Figure 1e). The difference between the mechanisms becomes even more important in the analysis of the dependence of photoemission on the nanoparticle shape and the direction of light incidence. It was shown that spatial asymmetry of nanocones gives rise to a preferred direction of photoemission under plasmonic resonance excitation. Such plasmonic photogalvanic effect exceeds its natural counterpart by several orders of magnitude.[32] It is natural to expect that this effect should be strongly affected by the balance between the photoemission mechanisms.

Thus, determining the individual contributions of bulk and surface photoemission mechanisms is an important task, merging purely theoretical studies[33−43] with experimental observation obtained up to now.[9,44−46] In this paper, we make a step toward bridging that gap and clarify the physical processes underlying the photoemission of hot electrons from plasmonic nanoparticles. We demonstrate that transition absorption is an important fundamental mechanism responsible for the energy transfer between the electromagnetic field and the electrons in the surface photoemission and consequently the increase in photoemission rate. We analytically study hot electron photoemission from spherical nanoparticles surrounded by different media and calculate the ratio of photoemission rates due to the surface and the bulk mechanisms. We show that the contribution of the surface mechanism cannot be neglected. The permittivity jump increases the role of the surface mechanism: it dominates for photon energies above 1−2 eV as, for example, for silicon, titanium dioxide, and zinc oxide interfacing with gold. Finally, we apply these results to analyze photoelectric processes in metallic nanowires deposited on top of a semiconductor substrate and partially embedded in it, which is of high practical relevance for narrow-band photodetection;[45] revisiting the results in ref 45, we show that they can be at least partially attributed to the surface photoemission effect.

DOI: 10.1021/acsphotonics.5b00059
ACS Photonics 2015, 2, 1039−1048

RESULTS

Transition Absorption and Its Contribution to the Surface Mechanism of Photoemission. Here we consider the process of transition absorption of a photon by an electron passing through an interface between two media with different permittivities. This phenomenon has not been thoroughly studied previously, but is naturally expected to take part in photoelectric processes involving metal−dielectric structures. One has to note that coherent stimulated transition radiation effects were studied earlier in view of the free-electron laser concept in relativistic electronics.[47−50] In those works, however, amplification of the plane wave incident normal to the interface between media was considered. In the present paper, we are interested in quite different interaction geometry of the surface plasmon electromagnetic wave.

Let us consider an electron passing through a flat boundary between different materials[51,52] in the presence of an electric field polarized *perpendicular* to the boundary.

Electric fields on each side of the boundary E_e and E_i with permittivities ε_e and ε_i, respectively, satisfy the relation (Figure 2)

$$\varepsilon_i E_i = \varepsilon_e E_e \tag{1}$$

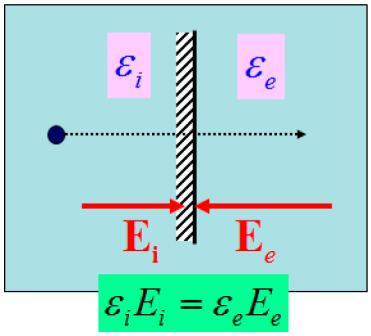

Figure 2. Classical electron passing through the boundary of two materials with different permittivities ε_e and ε_i.

The difference in the fields brought about by the permittivity step can cause the electron to change its velocity and, therefore, its kinetic energy. In the classical approximation, the energy change is

$$\Delta W_{\text{classic}} = \langle mv^2(+\infty)/2 - mv_0{}^2(-\infty)/2\rangle \tag{2}$$

where v_0 and v are initial and final velocity of the electron at an infinite distance from the boundary, m is the electron mass, and $\langle ...\rangle$ denotes the averaging over phase ϕ_i of the complex field amplitude $E_i = |E_i|e^{-i\phi_i}$. In this case, one can show that the energy absorbed by the electron is given by

$$\Delta W_{\text{classic}} = \frac{2e^2}{m\omega^2}|E_e - E_i|^2 = \frac{2e^2}{m\omega^2}|E_i|^2\left|\frac{\varepsilon_i}{\varepsilon_e} - 1\right|^2 \tag{3}$$

where ω is the frequency of the field oscillations and e is the electron charge. We refer to such loss of energy of an electron passing through an interface as "transition absorption".[52]

The same result can be obtained quantum mechanically. In this case,

$$\Delta W_{\text{quantum}} = \hbar\omega[p_+ - p_-] \tag{4}$$

Here p_+ and p_- are the probabilities of an electron of absorbing (and, respectively, emitting) a quantum $\hbar\omega$, given by

$$p_\pm = \frac{e^2 u_i}{2m\hbar^2\omega^4}\left(1 \pm \frac{\hbar\omega}{u_i}\right)^{-1/2}\left(1 + \sqrt{1 \pm \frac{\hbar\omega}{u_i}} \pm \frac{\hbar\omega}{2u_i}\right)^2 \times|E_e - E_i|^2 \tag{5}$$

where $u_i = \hbar^2 k_i^2/2m$ is the energy of an electron with wavenumber k_i. In the limit $\hbar\omega/u_i \ll 1$, eq 5 gives the classical formula 3. More detailed discussion and analysis of the process can be found in ref 52.

On the other hand, one can show that the rate of the electron emission from a metal nanoparticle into the surrounding semiconductor, as caused by the surface photoelectric effect, is given by[34]

$$R_{\text{em}}^{\text{surf}} = C_{\text{em}}^{\text{surf}}\int_{\text{surface}} \mathrm{d}s\,|E_i^{(n)}(\mathbf{r})|^2 = \eta_o\frac{2\varepsilon_o c}{\hbar\omega}\int_{\text{surface}} \mathrm{d}s\,|E_i^{(n)}(\mathbf{r})|^2 \tag{6}$$

where η_o is the external quantum efficiency of emission:

$$\eta_o = \frac{8}{\pi}\alpha_{\text{f-s}}\left(\frac{U_b}{\hbar\omega}\right)^3\int_{1-\hbar\omega/U_b}^{\varepsilon_F/U_b} \mathrm{d}X\,\mathrm{Re}\left[\sqrt{\left(X - 1 + \frac{\hbar\omega}{U_b}\right)}\right] \times\frac{G(X)}{\sqrt{X}}|K_{\Delta\varepsilon}(X)|^2\left(\frac{\varepsilon_F}{U_b} - X\right) \tag{7}$$

and

$$G(X) = X\frac{|\sqrt{X} - \sqrt{X-1}|^2}{|\sqrt{X + \hbar\omega/U_b} + \sqrt{X + \hbar\omega/U_b - 1}|^2} \tag{8}$$

$$K_{\Delta\varepsilon} = \frac{1}{2}\left[\left(\frac{\varepsilon_i}{\varepsilon_e} + 1\right) - \left(\frac{\varepsilon_i}{\varepsilon_e} - 1\right) \times\left(\sqrt{X + \frac{\hbar\omega}{U_b}} + \sqrt{X - 1}\right)^2\right] \tag{9}$$

Here, $X = u_i/U_b$ is the dimensionless kinetic energy, $U_b = W_b + \varepsilon_F$ is the potential jump at the interface, ε_F is the Fermi energy (we assume that $\hbar\omega < \varepsilon_F$), and $\alpha_{\text{f-s}} = e^2/(4\pi\varepsilon_o\hbar c) = 0.007297 - 1/137$ is the fine-structure constant.

We see from eqs 7−9 that the physical reason for transition absorption, namely, the difference between media permittivities of the two sides of the boundary, giving rise to different electric field strength in the two media as per eq 1, is also important in the derivation of the surface photoemission rate. Moreover, by comparing the expressions for transition absorption to those obtained earlier for the surface photoemission rate,[52] it can be shown that by transformation of eqs 7−9 in the approximation of $U_b = 0$, one can arrive at the result given by eq 5.

In order to further analyze the contribution of transition absorption to the surface photoemission, we compare the external quantum efficiency given by eq 7 to the quantity

$$\eta_o{}' = C(\lambda)\Delta W \tag{10}$$

where ΔW stands for either $\Delta W_{\text{classic}}$ or $\Delta W_{\text{quantum}}$, depending on the choice of the problem treatment. The phenomenological coefficient $C(\lambda)$ is introduced to provide the best match

DOI: 10.1021/acsphotonics.5b00059
ACS Photonics 2015, 2, 1039−1048

between η_o and ΔW for a given wavelength λ and consequently for a fixed value of metal permittivity. Indeed, Figure 3 shows

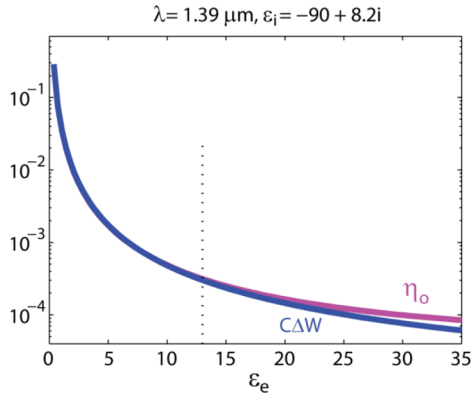

Figure 3. Comparison of external quantum efficiency η_o given by eq 7 and the account for the transition absorption only η_o' given by eq 10, for different permittivities of surrounding medium. Vertical dotted line corresponds to ε_e = 13, e.g., GaAs (the case studied in ref 34).

that in a broad range of permittivities of surrounding medium (broader than the practically available range for the sake of study), the relation 10 coincides with eq 7 rather well. A slight discrepancy between η_o' and η_o given by eqs 10 and 7, respectively, becomes more pronounced for $\varepsilon_e > 15$ (see Figure 3). This discrepancy indicates that another mechanism emerges in addition to transition absorption; namely, the electron loses energy to overcome the barrier with nonzero U_b.

Thus, we have shown that the transition absorption is the main effect that contributes to the surface mechanism of photoemission and causes an increase of the external quantum efficiency.

Influence of Permittivity Difference on Photoelectric Effect. As mentioned above, the surface and the bulk mechanisms were distinguished long ago, and theories for both of them were developed over the last 80 years.[18] In our earlier works, we showed that in a plasmonic nanoparticle both mechanisms have comparable contributions, and the surface one can dominate under some conditions.[34] It was shown that the ratio of contributions for the two mechanisms depends on the energy distribution of hot electrons, as well as on their cooling rate due to electron−electron collisions. Here we will apply these results to the case of nanoparticles and show the influence of the particle and surrounding matrix materials on the importance of the surface photoelectric effect.

A photoelectron emission process can be characterized by its cross-section, i.e., the ability of plasmonic nanoparticles to emit photoelectrons, given by

$$\sigma_{em} = R_{em}/(S/\hbar\omega) \tag{11}$$

where R_{em} is the rate of emission of photoelectrons from the nanoparticle, calculated, for example, by eq 6 for the surface photoelectric effect; a similar quantity can be introduced for the volume mechanism;[34] $S/\hbar\omega$ is the photon flux incident on the nanoparticle.

Relative contributions of the surface vs bulk mechanisms to the total photoemission rate can be characterized by a factor[34]

$$K_{S\text{-}B} = \frac{\sigma_{em}^{surf}}{\sigma_{em}^{bulk}} = \frac{\lambda}{2\pi a}\frac{\eta_o}{\varepsilon_i''\eta_i} \tag{12}$$

where

$$\sigma_{em}^{surf} = \frac{4\pi\eta_o}{3\sqrt{\varepsilon_e}}|F|^2 a^2 \tag{13}$$

and

$$\sigma_{em}^{bulk} = \frac{8\pi^2}{3}\frac{a}{\lambda}\frac{\varepsilon_i''}{\sqrt{\varepsilon_e}}|F|^2 a^2 \eta_i \tag{14}$$

are cross-sections for the surface and the bulk photoemission, respectively, a is the nanoparticle radius, η_o is the external

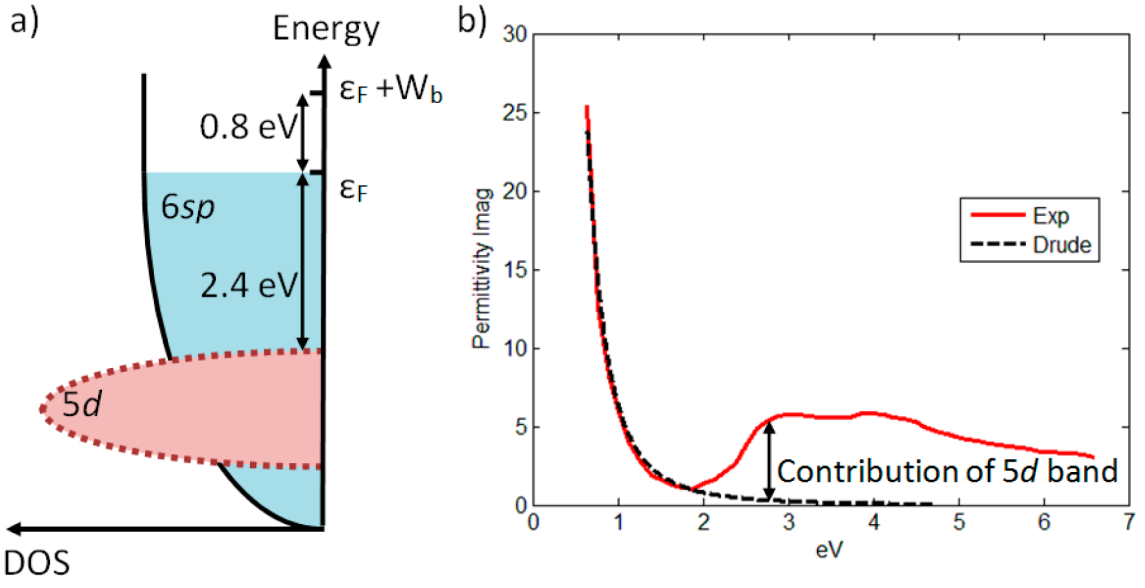

Figure 4. (a) Band structure of gold including the 5d-band, which lies 2.4 eV below the Fermi energy ε_F and consequently makes interband excitations considerably more unlikely than intraband excitations. (b) For the calculations, experimental data for gold permittivity from ref 53 are fitted by the Drude formula in the near-infrared range. The Drude fit excludes the contribution of interband transitions to Im ε_{Au} in the visible and ultraviolet ranges.

DOI: 10.1021/acsphotonics.5b00059
ACS Photonics 2015, 2, 1039−1048

quantum efficiency for the surface mechanism, η_i is the internal quantum efficiency for the bulk mechanism, $F = 3\varepsilon_e/(2\varepsilon_e + \varepsilon_i(\omega))$ is the enhancement of the field inside the nanoparticle (see ref 34), and $\varepsilon_i''(\omega)$ is the imaginary part of the metal permittivity $\varepsilon_i(\omega)$.

Note that in order to apply the formalism of ref 34 for the case of plasmonic nanoparticles in the relevant frequency ranges, the treatment of the bulk mechanism needs to be modified for the higher photon energies. Namely, the imaginary part of the metal permittivity needs to be adjusted to include only the contribution of "free" electrons, but not from interband transitions in the metal (see Figure 4), since electrons from the d-band require much higher energy to become hot, so they usually do not contribute to photoemission. Thus, the interband transition contribution must be removed from $\varepsilon_i''(\omega)$ during calculations of the light power absorbed inside the nanoparticle. For this reason, the calculations were performed with $\varepsilon_i(\omega)$ determined by the Drude model: $\varepsilon_i(\omega) = \varepsilon_\infty - \omega_{pl}^2/[\omega(\omega + i\gamma)]$ with $\varepsilon_\infty = 6.8$, $\omega_{pl} = 8.89$ eV, and $\gamma = 0.52$ eV.

We calculate the cross-sections for the surface σ_{em}^{surf} and the bulk σ_{em}^{bulk} photoemission (eqs 13 and 14, respectively) for gold (Au) spherical nanoparticles surrounded by p-type silicon (Si) to separate surface and bulk contributions as a function of energies. Figure 5a shows that the overall photoemission efficiency starts from zero at lower energy and then increases with increasing energy, up to a maximum value that corresponds to localized surface plasmon resonance on the nanoparticle. Further, we calculate $K_{B\text{-}S}$ for nanoparticles surrounded by different materials: Si, zinc oxide (ZnO), and titanium dioxide (TiO_2) (Figure 5b). The quantum-step-potential model was used for σ_{em}^{bulk} calculations. The work function from metal to semiconductor, i.e., the Schottky barrier height, was defined as $W_b = W_i - \chi$, where W_i is the work function of the metal and χ is the electron affinity of the semiconductor. The parameters are as follows: Au, $\varepsilon_F = 5.1$ eV, $W_i = 5.3$ eV, permittivity is taken from ref 53; Si, $\chi = 4.96$ eV, permittivity is approximated by the model from ref 33; ZnO, $\chi = 3.7$ eV from ref 54, permittivity is taken from ref 56; TiO_2, $\chi = 4.8$ eV from ref 55, permittivity is taken from ref 57. Neither a change of effective electron mass nor hole conductivity is taken into account. Electron collisions with the nanostructure boundary are taken into account following the approach in ref 58.

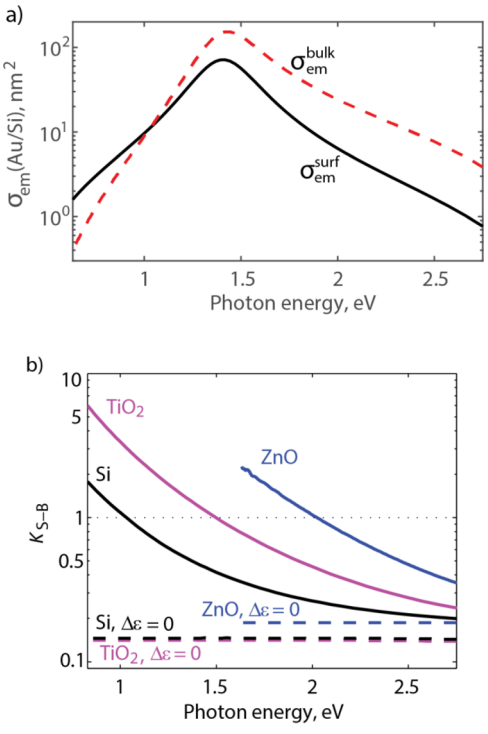

Figure 5. Comparison of surface and bulk mechanisms for gold nanospheres. (a) Separate contributions of the surface and bulk photoeffects show an overall decrease of the photoemission at low photon energies and a peak value at the frequency that corresponds to localized surface plasmon resonance. (b) Spectral dependence of the ratio $K_{S-B} = \sigma_{em}^{surf}/\sigma_{em}^{bulk}$ for different surrounding materials (Si, ZnO, and TiO_2). Nanosphere radius $a = 25$ nm. Calculations for the case where the difference in the permittivity of materials is artificially neglected (see text) are marked as $\Delta\varepsilon = 0$.

In general, photoemission strongly depends on the material quality, such as crystallinity and amount of defects. For semiconductors, the influence of bulk and surface defects was extensively studied (see, for example, refs 60 and 61), and in particular, decreasing the ratio of bulk defects to surface defects was found to significantly enhance the photocatalytic efficiency.[60] For metal films and nanoparticles, the presence of roughness and granularity influences the photoelectron emission in two ways. From one side, for nanoparticles, the smaller the size, the higher the ratio of surface to volume; that is, photoemission probability is higher.[41] The effect is similar to an increase in photoemission because of the surface roughness at the metal−semiconductor interface.[12] For small particles, the imaginary part of effective permittivity can be increased up to three times in comparison to bulk parameters $\tilde{\varepsilon}_i''(\omega) \approx 3\varepsilon_i''(\omega)$ because of the grains.[62] In turn, it increases absorption of photons inside the particles and photoemission (characterized by σ_{em}^{bulk}; see eq 14). From another side, because of the grains, the electron inside the nanoparticle experiences more collisions, and its effective mean free path l is decreased. Typical values of l are in a range 10−100 nm.[4,59] However, it was shown that for nanoparticles escape cone restriction is the most important, as nanoparticle size is on the order of or less than the mean free path.[4] For our calculations of the bulk mechanism photoemission cross-section, the mean free path for an electron inside the nanosphere was taken as $l = 41$ nm.[59]

Calculations show that the parameter $K_{S\text{-}B}$ can either be below unity (the bulk mechanism is dominant), exceed unity (the surface mechanism is prevalent), or be around 1 (which shows that both mechanisms need to be taken into account); the choice between these three cases depends on the materials and photon energies. We see that the surface mechanism becomes stronger below 2.0 eV for ZnO, 1.5 eV for TiO_2, and 1.0 eV for Si. Overall, Figure 5b shows that the surface mechanism gives a sizable contribution to the photoemission for photon energies below 1−2 eV and in a wide range of constituting materials. In some cases, the surface photoemission cross-section can be up to 10 times higher than the one for the bulk photoemission.

Furthermore, we have calculated $K_{S\text{-}B}$ in the special case of $\Delta\varepsilon = 0$, i.e., when the potential step at the nanoparticle boundary is retained but the permittivity step is artificially neglected. One can see in Figure 5b that for the model of step-like potential,[33,34] both σ_{em}^{surf} and σ_{em}^{bulk} are $\sim(\hbar\omega - W_b)^{5/2}$, and thus $K_{S\text{-}B,\Delta\varepsilon=0}$ almost does not depend on the wavelength. Moreover, $K_{S\text{-}B,\Delta\varepsilon=0}$ values are well below 1, which means that

DOI: 10.1021/acsphotonics.5b00059
ACS Photonics 2015, 2, 1039−1048

the bulk mechanism essentially dominates in this case. This additionally confirms that the permittivity step is of key importance in the surface photoelectric processes.

Influence of Nanoparticle and Surrounding Materials on the Surface Photoelectric Effect. In the first subsection, we have identified the transition absorption of a photon by an electron crossing a boundary between two different media and have shown that transition absorption gives a sizable contribution to the surface mechanism of photoemission. As the surface mechanism of photoemission is dominant for a particular spectral range and has important contributions from transition absorption, it motivates us to consider the surface mechanism in more detail.

From both Figure 3 and Figure 5b, one can see that the lower the surrounding permittivity ε_e, the higher η_o is (stemming from ε_e in the denominator of the expression for ΔW in eq 3), which suggests a way to increase photoemission from nanoparticles. Indeed, Figure 6 shows that for smaller

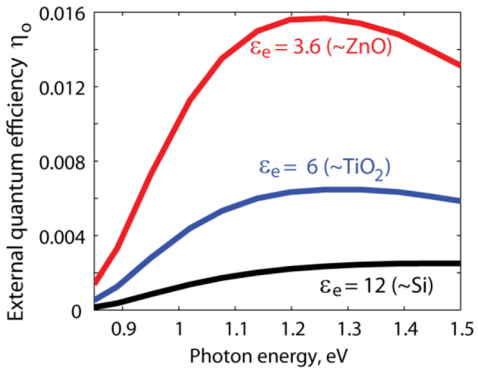

Figure 6. Spectral dependence of η_o for different permittivities of the surrounding medium. W_b is fixed at 0.8 eV.

permittivity, for instance ε_e = 6 or 3.6 (TiO_2 and ZnO, respectively), η_o is increased by several times compared to η_o for ε_e = 12. It should be mentioned that here (in contrast to Figure 5) we do not take into account the change of the barrier height for different materials assuming everywhere W_b = 0.8 eV, focusing only on the permittivity dependence of η_o.

Furthermore, the surface mechanism depends on the permittivity of the metal at the surface,[34] which therefore influences the photoemission rate. We calculate the external quantum efficiency of the photoemission η_o for Au/Si and Ti/Si interfaces (data for titanium (Ti) are taken from ref 63). Figure 7a shows that indeed η_o is several times higher for the Au/Si boundary than for the Ti/Si boundary. Ratios of ΔW and η_o for Au/Si and Ti/Si interfaces are increased for lower energies of photons (higher wavelength λ) and can reach up to 7 for λ = 1.9 μm (Figure 7b). In contrast to Au, Ti possesses a much lower absolute value of permittivity (see inset of Figure 7b). As one can predict from eq 3, the energy ΔW absorbed by an electron due to transition absorption on the Au/Si boundary is higher than on the Ti/Si boundary (plotted in Figure 7b), which results in the increase of photoemission. The mismatch between ratios of η_o and energy ΔW shown in Figure 7b is because the coefficient $C(\lambda)$ in eq 10 depends on the interface materials in addition to spectral dependence.

As the transition absorption gives a significant contribution to the surface mechanism of photoemission, increasing the difference between permittivities of the materials can lead to an additional photoemission enhancement. In particular, in the

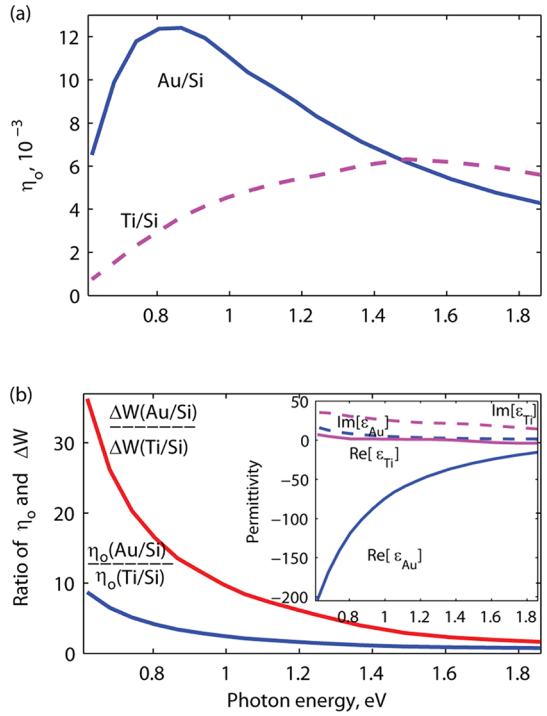

Figure 7. (a) External quantum efficiency of photoemission η_o for different nanoparticle materials. Photoemission from the Au/Si interface is much higher than for the Ti/Si interface. W_b = 0.5 eV is fixed. (b) Ratios of η_o and energies ΔW absorbed at transition absorption for different interfaces; the ratios are different due to material dependence of $C(\lambda)$ in eq 10. Inset: Permittivities of gold and titanium (experimental data from refs 53 and 63).

near-infrared range, the photoemission rate through the Au/Si boundary can be up to 7 times higher than through the Ti/Si boundary.

Surface Mechanism in Photoemission from Partially Embedded Plasmonic Nanowires. A recently performed experimental study[45] showed that photoemission from Au nanowires deposited on a silicon substrate and illuminated from the top is greatly increased when the nanowires are partially embedded into the substrate (Figure 8). At the same time, calculated absorption inside the structure turned out to be almost the same for different embedding depths D ranging from D_{min} = 5 nm to D_{max} = 25 nm. Moreover, because of the elongated shape of the nanowires (the nanowire width $w \gg D$), such embedding changes the total area of the photoemission-active surface only negligibly. Such change is referred to as geometric enhancement

$$g = \frac{2D_{max} + w}{2D_{min} + w} \tag{15}$$

Given that both absorption and the geometric surface variations are much weaker than the measured photocurrent increase, it becomes difficult to attribute that increase to the bulk photoemission mechanism. One possible explanation, proposed in ref 45, is based on the assumption that the excited hot electrons are distributed anisotropically in k-space, with more electrons having the momentum matching that of the incident photons; in turn, this causes an enhancement in charge injection over the vertical sidewalls of the embedded nanowires. Here we revisit the results of ref 45, mindful of the possible presence of the surface mechanism.

DOI: 10.1021/acsphotonics.5b00059
ACS Photonics 2015, 2, 1039−1048

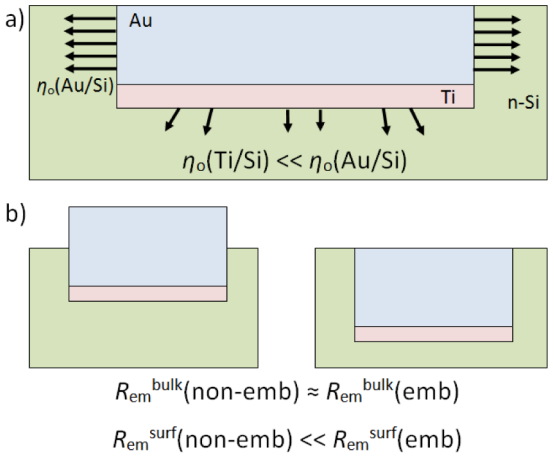

Figure 8. (a) Schematic view of a Au nanowire with a 2 nm thick adhesion layer of Ti used in the fabrication process. Different boundaries (Au/Si and Ti/Si) provide different rates of photoemission from the nanowire surface R_{em}^{surf}. (b) Embedding of a nanowire causes an increase of the Au/Si area and consequently an increase in total photoemission from it.

We note that the structure studied in ref 45 possesses a fabrication-related feature. During the fabrication process, a 2 nm thick adhesion layer of Ti was deposited by electron beam evaporation, which is a standard technique of adhesion improvement when depositing gold structures on silicon. High directionality of this deposition results in the situation where the bottom side has a Ti/Si interface, while the vertical sidewalls lack the Ti layer and have Au/Si boundaries (Figure 8a). Thus, the structure has two different interfaces, Au/Si and Ti/Si, and the area of only one of them is changing when the embedding depth varies. As was shown previously, permittivity of the metal strongly influences the photoemission rate (see Figure 7), and specifically, η_o is several times higher for the Au/Si boundary than for the Ti/Si boundary (Figure 8). Thus, when the embedding depth increases, the area of Au/Si photoemission also increases, while the area of weaker Ti/Si photoemission remains the same. As a result the total photocurrent can be expected to increase well beyond the geometrical enhancement factor g (eq 15).

It should be mentioned that single Ti atoms can end up on the vertical walls as well. Consequently, they can decrease the barrier height and allow photoemission from the whole surface area for photons with energies between 0.5 and 0.8 eV.

Following eq 6, in order to calculate the total surface-effect photoemission from nanowires, one needs to multiply η_o by the square of the normal component of the electric field $|E_n|^2$ and subsequently integrate over the whole area of contact between the nanowire and silicon, which consist of bottom wall and side walls:

$$R_{em}^{surf}(D) = \eta_o \frac{2\varepsilon_o c}{\hbar\omega} \int_{Emb.surf.[w+2D]} ds\,|E_n|^2 = \eta_o(\mathrm{Ti/Si}) \frac{2\varepsilon_o c}{\hbar\omega} \int_{bottow\ wall[w]} ds\,|E_n|^2 + \eta_o(\mathrm{Au/Si}) \frac{2\varepsilon_o c}{\hbar\omega} \int_{side\ walls[2D]} ds\,|E_n|^2 \quad (16)$$

We performed full simulations of electric field distribution in the nanowire array using the commercial package CST Microwave Studio. The permittivities of Au and Ti were taken from refs 53 and 63, respectively, and $\varepsilon_{Si} = 12$ was assumed. The corners of the Au nanowire and Ti layer were rounded with a curvature of 5 nm to suppress artificial "hot spots" and to bring the model system closer to reality.

We calculated photoemission for different embedding depths: D = 5, 15, and 25 nm (Figure 9). For each value of

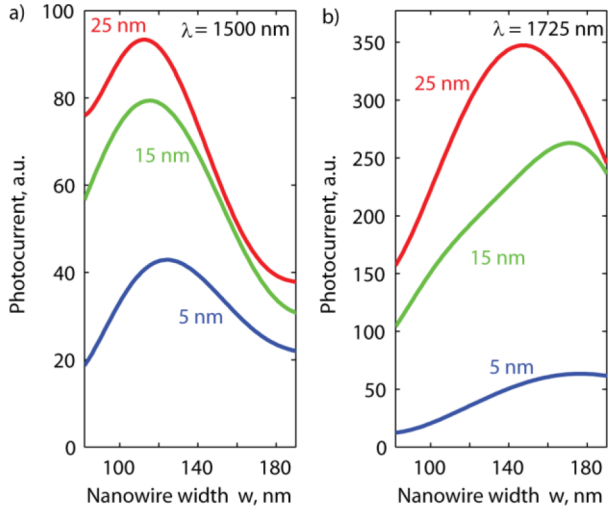

Figure 9. Calculations of photocurrent caused by photoemission from the nanoparticle surface. Similar to ref 45, embedding by 5, 15, and 25 nm is studied, and good qualitative agreement with experimental results of ref 45 is obtained. Wavelength is (a) 1500 nm and (b) 1725 nm.

D, there is a clear maximum at a certain nanowire width, and the total photocurrent increases as the nanowires become more embedded, which is in good qualitative agreement with experimental observation.[45] Note that quantitative agreement cannot be expected here because our calculations only take the surface photoelectric effect into account and because they contain a number of idealizations, neglecting the possible presence of defects either in the bulk or on the surface of the nanowires.

Further, we calculated the expected change of the photocurrent J due to the surface effect in the presence of two interface types,

$$s = \frac{J(D_{max})}{J(D_{min})} = \frac{R_{em}^{surf}(D_{max})}{R_{em}^{surf}(D_{min})} \quad (17)$$

and found a much higher increase than the "bare" geometric enhancement g (Figure 10). Comparing Figure 10 with Figure 9, we see that the increase of s results from the combined effect of the overall photocurrent increase for structures that are more deeply embedded and the accompanied shift of the nanowire width at which the resonance of photoemission occurs, so that the ratio in eq 17 becomes greater. Our calculations show that both effects can result from the surface photoelectric effect in the considered structure when just one detail of the fabrication process (namely, the presence of a Ti adhesion layer) is taken into account. Thus, one can see that the surface mechanism of photoemission can explain the observed photocurrent increase, even though the absorption in the nanowire is not increased accordingly, and thus photoemission from bulk Au should be the same for all embedding depths.

To conclude, we argue that the surface mechanism of photoemission shows up in the experimental results with

DOI: 10.1021/acsphotonics.5b00059
ACS Photonics 2015, 2, 1039−1048

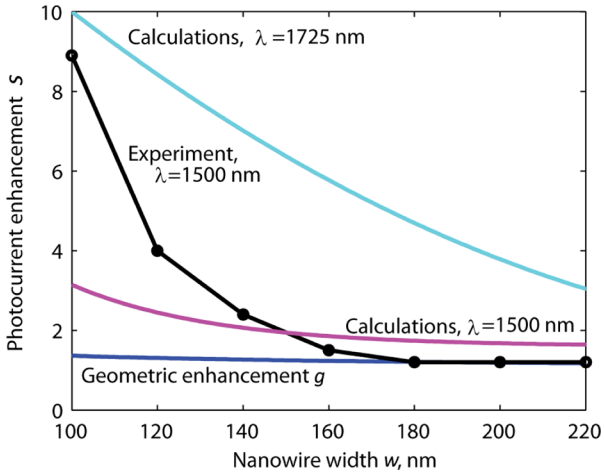

Figure 10. Comparison of enhancement of photocurrent in different cases. Geometric enhancement (approximately 1.5 times) does not explain the experimental results with up to a 10-fold increase. Conversely, the increase due to the surface mechanism s (eq 17, with D_{min} = 5 nm and D_{max} = 25 nm) reaches values of 3−5 for 1500 nm. Moreover, an even higher (up to 10-fold increase) value is obtained for a wavelength of 1725 nm, which corresponds to a resonance in the structure with a 500 nm period and a 3.45 refractive index of the substrate (silicon).

embedded nanowires and needs to be taken into account for an accurate explanation of the increase of photocurrent from nanowires embedded in a semiconductor as the embedding depth increases, as was observed experimentally in ref 45.

DISCUSSION

As mentioned above, the importance of the surface mechanism for photoemission processes dates back to the earlier works that considered flat metal films,[20−25] showing that the surface mechanism becomes significant (and even dominant) at the wavelength of the surface plasmon polariton excitation. In the nanoparticle scenario with *localized* surface plasmonic excitations, featuring enormous field enhancement in the regions of increased surface curvature, the photoemission is significantly enhanced in comparison to a flat metal surface.[41] Here we have shown, from a number of different standpoints, that the role of the surface mechanism is correspondingly more important in nanoparticles and nanostructures.

For the IR range, which is especially relevant for, for example, photodetector applications, our results confirm the previously obtained conclusion that most of the electrons are emitted from the surface of the nanoparticle rather than from its bulk part and that calculations of the photoemission rate definitely need to take the surface mechanism into account. For the localized plasmon resonance in the visible range (having solar cell applications in mind), the nanoparticle dimensions are smaller, increasing the probability that a hot electron excited inside the metal can reach its surface without energy loss, as compared to flat structures or larger nanoparticles. Nevertheless, it was shown recently that even if the mean free path of electrons is on the same order of magnitude as the size of the particle, the electrons may still fail to overcome the metal/surrounding interface.[4] This is because of limiting effects of the hot electron mean free path in conjunction with constraints on the escape cone and momentum conservation at the interface.

Recently, internal photoemission from metal films, nanowires, and nanospheres into a semiconductor was studied theoretically.[41] The jump of the effective electron mass at the metal−semiconductor interface and the cooling effect of hot electrons due to electron−electron collisions in the metal were taken into account. It was shown that the reduction of the effective mass of the electron during its transition from metal to semiconductor may lead to a significant—up to orders of magnitude—decrease in the internal quantum efficiency of bulk photoemission. Therefore, our conclusion is that the role of the surface photoelectric effect should not be underestimated even in cases where the volume mechanism was previously thought to be sufficient for the photoemission description. Generally, our conclusion is that it is unsafe to assume that either of the two mechanisms is dominant in the scenario as varied as the world of nanostructures, and both mechanisms must be taken into account.

Note that our analysis is purely theoretical and relies on the simulations of a somewhat idealized model of the nanoparticles. In particular, the effects brought about by defects and crystallinity in the plasmonic nanoparticles, as well as by surface roughness, are not considered. For example, it was previously shown that the presence of roughness on a flat metal surface can enable the light-induced drift and other kinetic effects[26] that would otherwise be forbidden by momentum conservation considerations, so the inclusion of surface roughness could make the surface photoeffect stronger. On the other hand, interfacial defects (especially at the metal/semiconductor interface) can severely decrease the hot electron injection, and it remains to be investigated which process—the surface or the volume one—is affected more strongly. For example, it was found earlier that decreasing the occurrence of bulk defects in TiO_2 nanocryctals can significantly improve photoemission-based photocatalysis.[60] Similarly effecting bulk and surface carrier recombination processes in semiconductor nanocrystal based water-splitting photocatalysts was found to increase the catalysis efficacy.[61] It remains an open question, and a subject for future research, whether such separate control over bulk and surface defects can optimize photoelectron emission in plasmonic nanostructures.

We believe that our findings will help to underlie fundamental processes behind photoelectric and photochemical phenomena in plasmonic nanoparticles and nanostructures. As such, our results can be applied in all areas where nanoparticles and nanoantennas are employed to locally modify optical and chemical processes. The field of plasmon-assisted photocurrent generation is the subject of avid research and rapid development, as it is of high importance to both new photodetector technologies and solar energy harvesting. Much more remains to be investigated in this interesting topic, both experimentally and theoretically, e.g., probing the photoelectric effects in nanostructures of varied materials and geometry. New schemes for solar energy conversion, based on tailoring the surface and the volume photoelectric effects individually, will enable a way to realize photovoltaic and photocatalytic devices that may outperform conventional devices in terms of efficiency and/or versatility.

CONCLUSION

To summarize, we have considered the role of the surface photoelectric effect in plasmon-assisted hot electron generation in nanostructures from several important standpoints. First, we made a comparison of the surface mechanism and transition absorption, which occurs when an electron passes a boundary between two media with different permittivities, and confirmed

DOI: 10.1021/acsphotonics.5b00059
ACS Photonics 2015, 2, 1039−1048

that the latter is responsible for the increase of photoemission attributable to the surface photoelectric effect. Second, we compared photoemission from spherical plasmonic nanoparticles attributed to two physical mechanisms (electron photoemission from the surface and from the bulk of the nanoparticle) and showed that the surface mechanism is significant and even prevalent in the near-infrared range. Third, we analyzed the influence of material parameters on the increase of photoemission caused by transition absorption. Finally, we drew a parallel between the surface mechanism of photoemission and experimental results of ref 45 recently observed for partially embedded nanowires in a semiconductor. We showed that even if light absorption in the plasmonic nanowire remains the same so that the bulk mechanism should provide a constant photoemission rate, the surface mechanism can be responsible for photoemission enhancement if different materials are involved in a nanostructure and if their interface area is changed with respect to each other.

AUTHOR INFORMATION

Corresponding Authors

*E-mail: v.babicheva@phoi.ifmo.ru.
*E-mail: alexusk@lebedev.ru.

Notes

The authors declare no competing financial interest.

ACKNOWLEDGMENTS

V.E.B. acknowledges financial support from SPIE Optics and Photonics Education Scholarship and Kaj og Hermilla Ostenfeld Foundation. S.V.Z. acknowledges partial financial support from the People Programme (Marie Curie Actions) of the European Union's 7th Framework Programme FP7-PEOPLE-2011-IIF under REA grant agreement No. 302009 (Project HyPHONE). The authors acknowledge the Russian Foundation for Basic Research (Grant No. 13-08-01438) for financial support.

REFERENCES

(1) Clavero, C. Plasmon-Induced Hot-Electron Generation at Nanoparticle/Metal-Oxide Interfaces for Photovoltaic and Photocatalytic Devices. *Nat. Photonics* **2014**, *8*, 95−103.
(2) White, T. P.; Catchpole, K. R. Plasmon-Enhanced Internal Photoemission for Photovoltaics: Theoretical Efficiency Limits. *Appl. Phys. Lett.* **2012**, *101*, 073905.
(3) Novitsky, A.; Uskov, A.; Gritti, C.; Protsenko, I. E.; Kardynal, B.; Lavrinenko, A. Photon Absorption and Photocurrent in Solar Cells Below Semiconductor Bandgap Due to Electron Photoemission from Plasmonic Nanoantennas. *Prog. Photovoltaics* **2014**, *22*, 422−426.
(4) Leenheer, A. J.; Narang, P.; Lewis, N. S.; Atwater, H. A. Solar Energy Conversion Via Hot Electron Internal Photoemission in Metallic Nanostructures: Efficiency Estimates. *J. Appl. Phys.* **2014**, *115*, 134301.
(5) Mubeen, S.; Lee, J.; Lee, W.; Singh, N.; Stucky, G. D.; Moskovits, M. On the Plasmonic Photovoltaic. *ACS Nano* **2014**, *8*, 6066−6073.
(6) Mubeen, S.; Hernandez-Sosa, G.; Moses, D.; Lee, J.; Moskovits, M. Plasmonic Photosensitization of a Wide Band Gap Semiconductor: Converting Plasmons to Charge Carriers. *Nano Lett.* **2011**, *11*, 5548−5552.
(7) Berini, P. Surface Plasmon Photodetectors and Their Applications. *Laser Photonics Rev.* **2014**, *8*, 197−220.
(8) Moskovits, M. Hot Electrons Cross Boundaries. *Science* **2011**, *332*, 676.
(9) Knight, M. W.; Sobhani, H.; Nordlander, P.; Halas, N. J. Photodetection with Active Optical Antennas. *Science* **2011**, *332*, 702.
(10) Chalabi, H.; Schoen, D.; Brongersma, M. L. Hot-Electron Photodetection with a Plasmonic Nanostripe Antenna. *Nano Lett.* **2014**, *14*, 1374−1380.
(11) Goykhman, I.; Desiatov, B.; Khurgin, J.; Shappir, J.; Levy, U. Locally Oxidized Silicon Surface-Plasmon Schottky Detector for Telecom Regime. *Nano Lett.* **2011**, *11*, 2219−2224.
(12) Goykhman, I.; Desiatov, B.; Khurgin, J.; Shappir, J.; Levy, U. Waveguide Based Compact Silicon Schottky Photodetector with Enhanced Responsivity in the Telecom Spectral Band. *Opt. Express* **2012**, *20*, 28594−28602.
(13) Aruda, K. O.; Tagliazucchi, M.; Sweeney, C. M.; Hannah, D. C.; Weiss, E. A. The Role of Interfacial Charge Transfer-Type Interactions in the Decay of Plasmon Excitations in Metal Nanoparticles. *Phys. Chem. Chem. Phys.* **2013**, *15*, 7441−7449.
(14) Chalabi, H.; Brongersma, M. L. Plasmonics: Harvest Season for Hot Electrons. *Nat. Nanotechnol.* **2013**, *8*, 229−230.
(15) Mubeen, S.; Lee, J.; Singh, N.; Krämer, S.; Stucky, G. D.; Moskovits, M. An Autonomous Photosynthetic Device in Which All Charge Carriers Derive from Surface Plasmons. *Nat. Nanotechnol.* **2013**, *8*, 247−251.
(16) Lee, J.; Mubeen, S.; Ji, X.; Stucky, G. D.; Moskovits, M. Plasmonic Photoanodes for Solar Water Splitting with Visible Light. *Nano Lett.* **2012**, *12*, 5014−5019.
(17) Thomann, I.; Pinaud, B. A.; Chen, Z.; Clemens, B. M.; Jaramillo, B. M.; Brongersma, M. L. Plasmon Enhanced Solar-To-Fuel Energy Conversion. *Nano Lett.* **2011**, *11*, 3440−3446.
(18) Tamm, I.; Schubin, S. Zur Theorie des Photoeffektes an Metallen. *Eur. Phys. J. A* **1931**, *68*, 97−113.
(19) Afanas'ev, V. V. *Internal Photoemission Spectroscopy. Principles and Applications*; Elsevier, 2008.
(20) Brodsky, A. M.; Gurevich, Y. Y. Theory of External Photoeffect from the Surface of a Metal. *Sov. Phys. JETP* **1968**, *27*, 114−121.
(21) Brodsky, A. M.; Gurevich, Y. Y. *Theory of Electron Emission from Metals*; Nauka: Moscow, 1973.
(22) Glasser, M. L.; Bagchi, A. Theories of Photoemission from Metal Surfaces. *Prog. Surf. Sci.* **1976**, *7*, 113−148.
(23) Endriz, J. G. Calculation of the Surface Photoelectric Effect. *Phys. Rev. B* **1973**, *7*, 3464.
(24) Endriz, J. G.; Spicer, W. E. Experimental Evidence for the Surface Photoelectric Effect in Aluminum. *Phys. Rev. Lett.* **1971**, *27*, 570.
(25) Callcott, T. A.; Arakawa, E. T. Volume and Surface Photoemission Processes from Plasmon Resonance Fields. *Phys. Rev. B* **1975**, *11*, 2750.
(26) Shalaev, V. M.; Douketis, C.; Stuckless, J. T.; Moskovits, M. Light-Induced Kinetic Effects in Solids. *Phys. Rev. B: Condens. Matter Mater. Phys.* **1996**, *53*, 11388.
(27) Wang, F.; Melosh, N. A. Power-Independent Wavelength Determination by Hot Carrier Collection in Metal-Insulator-Metal Devices. *Nat. Commun.* **2013**, *4*, 1711.
(28) Sheldon, M. T.; van de Groep, J.; Brown, A. M.; Polman, A.; Atwater, H. A. Plasmoelectric Potentials in Metal Nanostructures. *Science* **2014**, *346*, 828.
(29) Brongersma, M. L.; Halas, N. J.; Nordlander, P. Plasmon-Induced Hot Carrier Science and Technology. *Nat. Nanotechnol.* **2015**, *10*, 25−34.
(30) Dalal, V. L. Simple Model for Internal Photoemission. *J. Appl. Phys.* **1971**, *42*, 2274.
(31) Stuart, R.; Wooten, F.; Spicer, W. E. Monte Carlo Calculations Pertaining to the Transport of Hot Electrons in Metals. *Phys. Rev.* **1964**, *135*, A495.
(32) Zhukovsky, S. V.; Babicheva, V. E.; Evlyukhin, A. B.; Protsenko, I. E.; Lavrinenko, A. V.; Uskov, A. V. Giant Photogalvanic Effect in Noncentrosymmetric Plasmonic Nanoparticles. *Phys. Rev. X* **2014**, *4*, 031038.
(33) Protsenko, I. E.; Uskov, A. V. Photoemission from Metal Nanoparticles. *Phys.-Usp.* **2012**, *55*, 508.
(34) Uskov, A. V.; Protsenko, I. E.; Ikhsanov, R. Sh.; Babicheva, V. E.; Zhukovsky, S. V.; Lavrinenko, A. V.; O'Reilly, E. P.; Xu, H. Internal

DOI: 10.1021/acsphotonics.5b00059
ACS Photonics 2015, 2, 1039−1048

Photoemission from Plasmonic Nanoparticles: Comparison between Surface and Volume Photoelectric Effects. *Nanoscale* **2014**, *6*, 4716−4727.
(35) Govorov, A. O.; Zhang, H.; Gun'Ko, Y. K. Theory of Photoinjection of Hot Plasmonic Carriers from Metal Nanostructures into Semiconductors and Surface Molecules. *J. Phys. Chem. C* **2013**, *117*, 16616−16631.
(36) Zhang, H.; Govorov, A. O. Optical Generation of Hot Plasmonic Carriers in Metal Nanocrystals: The Effects of Shape and Field Enhancement. *J. Phys. Chem. C* **2014**, *118*, 7606−7614.
(37) Govorov, A. O.; Zhang, H.; Demir, H. V.; Gun'ko, Y. K. Photogeneration of Hot Plasmonic Electrons with Metal Nanocrystals: Quantum Description and Potential Applications. *Nano Today* **2014**, *9*, 85−101.
(38) Manjavacas, A.; Liu, J. G.; Kulkarni, V.; Nordlander, P. Plasmon-Induced Hot Carriers in Metallic Nanoparticles. *ACS Nano* **2014**, *8*, 7630−7638.
(39) Sundararaman, R.; Narang, P.; Jermyn, A. S.; Goddard, W. A., III; Atwater, H. A. Theoretical Predictions for Hot-Carrier Generation from Surface Plasmon Decay. *Nat. Commun.* **2014**, *5*, 5788.
(40) Ikhsanov, R. Sh.; Protsenko, I. E.; Uskov, A. V.; Guzhva, M. E. Dependence of the Electron Photoemission from Metallic Nanoparticles on Their Size. *J. Russ. Laser Res.* **2014**, *35*, 501−508.
(41) Ikhsanov, R. Sh.; Babicheva, V. E.; Protsenko, I. E.; Uskov, A. V. Bulk Photoemission from Metal Films and Nanoparticles. *Quantum Electron.* **2015**, *45*, 50−58.
(42) Zhukovsky, S. V.; Babicheva, V. E.; Uskov, A. V.; Protsenko, I. E.; Lavrinenko, A. V. Enhanced Electron Photoemission by Collective Lattice Resonances in Plasmonic Nanoparticle-Array Photodetectors and Solar Cells. *Plasmonics* **2014**, *9*, 283−289.
(43) Zhukovsky, S. V.; Babicheva, V. E.; Uskov, A. V.; Protsenko, I. E.; Lavrinenko, A. V. Electron Photoemission in Plasmonic Nanoparticle Arrays: Analysis of Collective Resonances and Embedding Effects. *Appl. Phys. A: Mater. Sci. Process.* **2014**, *116*, 929−940.
(44) Sobhani, A.; Knight, M. W.; Wang, Y.; Zheng, B.; King, N. S.; Brown, L. V.; Fang, Z.; Nordlander, P.; Halas, N. J. Narrowband Photodetection in the Near-Infrared with a Plasmon-Induced Hot Electron Device. *Nat. Commun.* **2013**, *4*, 1643.
(45) Knight, M. W.; Wang, Y.; Urban, A. S.; Sobhani, A.; Zheng, B. Y.; Nordlander, P.; Halas, N. J. Embedding Plasmonic Nanostructure Diodes Enhances Hot Electron Emission. *Nano Lett.* **2013**, *13*, 1687−1692.
(46) Ishii, S.; Inoue, S.; Ueda, R.; Otomo, A. Optical Detection in a Waveguide Geometry with a Single Metallic Contact. *ACS Photonics* **2014**, *1*, 1089−1092.
(47) Arutyunyan, V. M.; Oganesyan, S. G. Interaction of Charged Particles with Strong Monochromatic Radiation in an Inhomogeneous Medium. *Sov. Phys. JETP* **1977**, *45*, 244−246.
(48) Oganesyan, S. G.; Engibaryan, V. A. Amplification of an Electromagnetic Wave by a Beam of Electrons at an Interface Between Two Media. *Sov. J. of Quantum Electron.* **1980**, *10*, 1283.
(49) Piestrup, M. A.; Finman, P. F. The Prospects of an X-Ray Free Electron Laser Using Stimulated Resonance Transition Radiation. *IEEE J. Quantum Electron.* **1983**, *19*, 357.
(50) Datta, S.; Kaplan, A. E. Quantum Theory of Spontaneous and Stimulated Resonant Transition Radiation. *Phys. Rev. A: At., Mol., Opt. Phys.* **1985**, *31*, 790.
(51) Ginzburg, V. L.; Motulevich, G. P. Optical Properties of Metals. *Usp. Fiz. Nauk* **1955**, *55*, 469−535.
(52) Uskov, A. V. ; Smetanin, I. V.; Protsenko, I. E.; Ikhsanov, R. Sh; Zhukovsky, S. V.; Babicheva, V. E. *Transition Absorption As a Mechanism of Surface Photoelectron Emission from Metals*. http://arxiv.org/abs/1412.1935, 2014.
(53) Johnson, P. B.; Christy, R. W. Optical Constants of the Noble Metals. *Phys. Rev. B* **1972**, *6*, 4370−4379.
(54) Jacobi, K.; Zwicker, G.; Gutmann, A. Work Function, Electron Affinity and Band Bending of Zinc Oxide Surfaces. *Surf. Sci.* **1984**, *141*, 109−125.
(55) Scanlon, D. O.; Dunnill, C. W.; Buckeridge, J.; Shevlin, S. A.; Logsdail, A. J.; Woodley, S. M.; Catlow, C. R. A.; Powell, M. J.; Palgrave, R. G.; Parkin, I. P.; et al. Band Alignment of Rutile and Anatase TiO_2. *Nat. Mater.* **2013**, *12*, 798−801.
(56) Bond, W. L. Measurement of the Refractive Indices of Several Crystals. *J. Appl. Phys.* **1965**, *36*, 1674−1677.
(57) Devore, J. R. Refractive Indices of Rutile and Sphalerite. *J. Opt. Soc. Am.* **1951**, *41*, 416−419.
(58) Uskov, A. V.; Protsenko, I. E.; Mortensen, N. A.; O'Reilly, E. P. Broadening of Plasmonic Resonance Due to Electron Collisions with Nanoparticle Boundary: a Quantum Mechanical Consideration. *Plasmonics* **2014**, *9*, 185−192.
(59) Frese, K. W., Jr.; Chen, C. Theoretical Models of Hot Carrier Effects at Metal-Semiconductor Electrodes. *J. Electrochem. Soc.* **1992**, *139*, 3234.
(60) Kong, M.; Li, Y.; Chen, X.; Tian, T.; Fang, P.; Zheng, F.; Zhao, X. Tuning the Relative Concentration Ratio of Bulk Defects to Surface Defects in TiO_2 Nanocrystals Leads to High Photocatalytic Efficiency. *J. Am. Chem. Soc.* **2011**, *133*, 16414−16417.
(61) Appavoo, K.; Liu, M.; Black, C. T.; Sfeir, M. Y. Quantifying Bulk and Surface Recombination Processes in Nanostructured Water Splitting Photocatalysts via in situ Ultrafast Spectroscopy. *Nano Lett.* **2015**, *15*, 1076−1082.
(62) Chen, K. P.; Drachev, V. P.; Borneman, J. D.; Kildishev, A. V.; Shalaev, V. M. Drude Relaxation Rate in Grained Gold Nanoantennas. *Nano Lett.* **2010**, *10*, 916−922.
(63) Ordal, M. A.; Bell, R. J.; Alexander, R. W.; Newquist, L. A.; Querry, M. R. Optical Properties of Al, Fe, Ti, Ta, W, and Mo at Submillimeter Wavelengths. *Appl. Opt.* **1988**, *27*, 1203−1209.

DOI: 10.1021/acsphotonics.5b00059
ACS Photonics 2015, 2, 1039−1048